
Contextual Memory Trees

Wen Sun¹ Alina Beygelzimer² Hal Daumé III³ John Langford³ Paul Mineiro⁴

Abstract

We design and study a Contextual Memory Tree (CMT), a learning *memory controller* that inserts new memories into an *experience store* of unbounded size. It is designed to efficiently query for *memories* from that store, supporting logarithmic time insertion and retrieval operations. Hence CMT can be integrated into existing statistical learning algorithms as an augmented memory unit without substantially increasing training and inference computation. Furthermore CMT operates as a reduction to classification, allowing it to benefit from advances in representation or architecture. We demonstrate the efficacy of CMT by augmenting existing multi-class and multi-label classification algorithms with CMT and observe statistical improvement. We also test CMT learning on several image-captioning tasks to demonstrate that it performs computationally better than a simple nearest neighbors memory system while benefiting from reward learning.

1. Introduction

When a human makes a decision or answers a question, they are able to do so while very quickly drawing upon a lifetime of remembered experiences. This ability to retrieve relevant experiences efficiently from a memory store is currently lacking in most machine learning systems (§1.1). We consider the problem of learning an efficient online data structure for use as an external memory in a reward-driven environment. The key functionality of the Contextual Memory Tree (CMT) data structure defined here is the ability to *insert* new memories into a learned key-value store, and to be able to *query* those memories in the future. The storage and query functionality in CMT is driven by an optional, user-specified, external reward signal; it organizes memories so as to maximize the downstream reward of queries.

¹School of Computer Science, Carnegie Mellon University, USA ²Yahoo! Research, New York, NY, USA ³Microsoft Research, New York, NY, USA ⁴Microsoft, USA. Correspondence to: Wen Sun <wensun@cs.cmu.edu>.

In order to scale to very large memories, our approach organizes memories in a tree structure, guaranteeing logarithmic time (in the number of memories) operations throughout (§3). Because CMT operates as a reduction to classification, it does not prescribe a representation for the keys and can leverage future advances in classification techniques.

More formally, we define the data structure CMT (§2), which converts the problem of mapping *queries* (keys) to *memories* (key-value pairs) into a collection of classification problems. Experimentally (§4), we show this is useful in three different settings. **(a)** Few-shot learning in extreme multiclass classification problems, where CMT is used directly as a classifier (the queries are examples and the values are class labels). Figure 1 shows that *unsupervised* CMT can statistically outperform other *supervised* logarithmic-time baselines including LOMTree (Choromanska & Langford, 2015) and Recall Tree (RT) (Daumé et al., 2017) with supervision providing further improvement. **(b)** Extreme multi-label classification problems where CMT is used to augment a One-Against-All (OAA) style inference algorithm. **(c)** Retrieval of images based on captions, where CMT is used similarly to a nearest-neighbor retrieval system (the queries are captions and the values are the corresponding images). External memories that persist across examples are also potentially useful as inputs to downstream applications; for instance, in natural language dialog tasks (Bartl & Spanakis, 2017) and in machine translation (Gu et al., 2018), it can be useful to retrieve similar past contexts (dialogs or documents) and augment the input to the downstream system with these retrieved examples. Memory-based systems can also be useful as a component of learned reasoning systems (Weston et al., 2014; Graves et al., 2016).

A memory $z = (x, \omega)$ is a pair of query x and value ω . CMT operates in the following generic online manner, repeated over time:

1. Given a query x , retrieve k associated memories $(u, \langle z_1, z_2, \dots, z_k \rangle) = \text{QUERY}(x)$ together with an identifier u .
2. If a reward r_i for z_i is observed, update the system via $\text{UPDATE}((x, z_i, r_i), u)$.
3. If a value ω associated with x is available, INSERT a new memory $z = (x, \omega)$ into the system.

A natural goal in such a system is a notion of self-

	Low Time	Small Space	Self-consistent	Incremental	Learning
Inverted Index		✓	✓		
Supervised Learning	✓	✓		✓	✓
Nearest Neighbor		✓	✓	✓	
Approx-NN	✓	✓	✓		
Learned-NN		✓	✓		✓
Hashing		✓	✓		✓
Differentiable Memory		✓	✓	✓	✓
CMT	✓	✓	✓	✓	✓

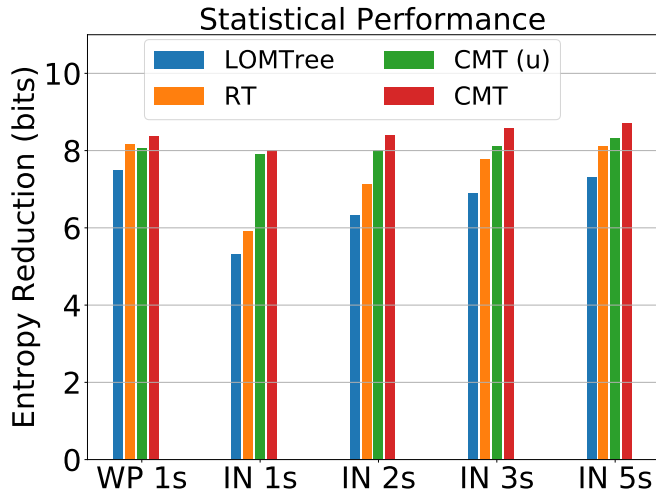


Figure 1: (Left) Desiderata satisfied by prior approaches; where answers vary with choices, we default towards ‘yes’. (Right) Statistical performance (Entropy Reduction from the constant predictor. Higher is better—see the experiments section.) on WikiPara one-shot (WP 1s) dataset and ImageNet S -shot datasets (IN S s) with baselines (LOMTree and RecallTree) and our proposed approach (unsupervised and supervised) CMT.

consistency. If the system inserts $z = (x, \omega)$ into CMT, then in subsequent rounds, one should expect that (x, ω) is retrieved when $\text{QUERY}(x)$ is issued again for the same x . (For simplicity, we assume that all x are unique.) In order to achieve such self-consistency in a data structure that changes over time, we augment CMT with a ‘‘Reroute’’ operation, in which the data structure gradually reorganizes itself by removing old memories and re-inserting them on an amortized basis. We find that this Reroute operation is essential to good empirical performance (§4.5).

1.1. Existing Approaches

The most standard associative memory system is a map data structure (e.g., hashmap, binary tree, relational database); unfortunately, these do not *generalize* across inputs—either an input is found exactly or it is not. We are interested in memories that can generalize beyond exact lookups, and can *learn* to do so based on past successes and failures in an *incremental*, online manner. Because we wish to scale, the *computation time* for all operations must be at most logarithmic in the number of memories, with *constant space overhead* per key-value pair. Finally, as mentioned above, such a system should be *self-consistent*.

There are many existing approaches beyond hashmaps, all of which miss one of our desiderata (Figure 1). A basic approach for text documents is an **inverted index** (Knuth, 1997; Broder et al., 2003), which indexes a document by the words that appear therein. On the other end of the spectrum, **supervised learning** can be viewed as remembering (compiling) a large amount of experience into a predictor which may offer very fast evaluation, but generally cannot

explicitly query for past memories (aka examples).

There has been substantial recent interest in coupling neural networks with nearest neighbor variants. Classical approaches are inadequate: **a) Exact nearest neighbor** algorithms (including memory systems that use them (Kaiser et al., 2017)) are computationally inefficient except in special cases (Dasgupta & Sinha, 2015; Beygelzimer et al., 2006) and do not learn. **b) Approximate Nearest Neighbors** via Locality-Sensitive Hashing (Datar et al., 2004) and MIPS (Shrivastava & Li, 2015) address the problem of computational time, but not learning. **c) Nearest Neighbors with Learned Metrics** (Weinberger et al., 2005) can learn, but are non-incremental.

More recent results combine neural architectures with forms of approximate nearest neighbor search to address these shortcomings. For example, (Rae et al., 2016) uses a representation learned for a task with either randomized kd-trees or locality sensitive hashing on a pre-existing (Euclidean distance) metric, both of which are periodically recomputed. The CMT instead learns at *individual nodes* and works for *any* representation. The CMT therefore avoids presupposing that a Euclidean metric is appropriate and could potentially productively replace the approximate nearest neighbor subsystem here.

Similarly, (Chandar et al., 2016) experiments with a variety of K-MIPS (Maximum Inner Product Search) data structures which the memory tree could potentially replace to create a higher ceiling on performance in situations where MIPS is not the right notion of similarity.

In (Andrychowicz & Kurach, 2016) the authors learn a hier-

archical data structure over a pre-partitioned set of memories with a parameterized JOIN operator shared across nodes. The use of pre-partition makes the data structure particularly sensitive to the (unspecified) order of that prepartition as discussed in appendix 6 of the LOMTree (Choromanska & Langford, 2015). Furthermore, tying the parameters of JOIN across the nodes deeply constrains the representation compared to our approach.

Many of these shortcomings are addressed by **learned hashing**-based models (Salakhutdinov & Hinton, 2009; Rastegari et al., 2012), which learn a hash function that works well at prediction time, but all current approaches are non-incremental and require substantial training-time overhead. Finally, **differentiable memory systems** (Weston et al., 2014; Graves et al., 2016) are able to refine memories over time, but rely on gradient-descent-based techniques which incur a computational overhead that is inherently linear in the number of memories.

2. The Contextual Memory Tree

At a high level, a CMT (Figure 2) is a near-balanced binary tree whose size dynamically increases as more memories are inserted. All memories are stored in leaf nodes with each leaf containing at most $c \log n$ memories, where n is the total number of memories and c is a constant independent of the number of memories.

Learning happens at every node of CMT. Each internal node contains a learning router. Given a query, CMT routes from the root to a leaf based on left-or-right decisions made by the routers along the way. Each internal node optimizes a metric, which ensures both its router’s ability to predict which sub-tree contains the best memory corresponding to the query, and the balance between its left and right subtrees. CMT also contains a global learning scorer that predicts the reward of a memory for a query. The scorer is used at a leaf to decide which memories to return, with updates based on an external reward signal of memory quality.

The rest of the section gives a detailed description of the data structure and the algorithms.

2.1. Data Structures

A *memory* consists of a *query* (key) $x \in \mathcal{X}$ and its associated *value* $\omega \in \Omega$. We use z to denote the memory pair (x, ω) and define $\mathcal{Z} = \mathcal{X} \times \Omega$ as the set of z . Given a memory z , we use $z.x$ and $z.\omega$ to represent the query and the value of z respectively. For instance, for multiclass classification, x is a feature vector and ω is a label. Our memory store is organized into a binary tree. A *leaf* node in Figure 3 (left top) consists of a parent and a set of memories. Leaf nodes are connected by internal nodes as in Figure 3 (left, bottom). An internal node has a parent and two children,

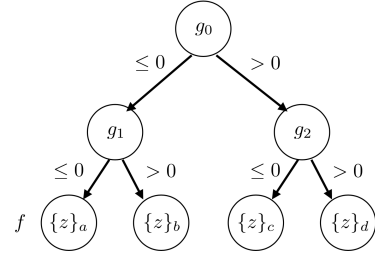


Figure 2: An example of CMT, where each internal node contains a binary classifier g as the router, and every leaf stores a small set of memories $\{z\}$. All leafs share a learning scorer f which computes a score of a memory z and a query x , and is used to select a memory when a query reaches a leaf.

which may be either leaf or internal nodes, a count n of the number of memories beneath the node, and a learning router $g : \mathcal{X} \rightarrow \{-1, 1\}$ which both routes via $g(x)$ and updates via $g.update(x, y)$ for $y \in \{-1, 1\}$, or $g.update(x, y, i)$ where $i \in \mathbb{R}^+$ is an importance weight of (x, y) . If $g(x) \leq 0$, we route x left, and otherwise right.

The contextual memory tree data structure in Figure 3 (right) has a root node, a parameter $\alpha \in [0, 1]$ which controls how balanced the tree is, a multiplier c on the maximum number of memories stored in any single leaf node, and a learning scorer $f : \mathcal{X} \times \mathcal{Z} \rightarrow \mathbb{R}$. Given a query x and memory z , the learning scorer predicts the reward one would receive if z is returned as the retrieved memory for query x via $f(x, z)$. Once a reward $r \in [0, 1]$ is received for a pair of memory z and query x , the learning scorer updates via $f.update(x, z, r)$ to improve its ability to predict reward. Finally, the map M maps examples to the leaf that contains them, making removal easy.

Given any internal node v and query x , we define a data structure path representing the path taken from v to a leaf: $path = \{(v_i, a_i, p_i)\}_{i=1}^N$, where $v_1 = v$, $a_i \in \{\text{left}, \text{right}\}$ is the left or right decision made at v_i , $p_i \in [0, 1]$ is the probability with which a_i was chosen. As we show later, path communicates to the update rule the information needed to create an unbiased update of routers.

2.2. Algorithms

All algorithms work given a contextual memory tree T . For brevity, we drop T when referencing its fields. We use $\in_U P$ to chose uniformly at random from a set P .

Algorithm 1 (PATH) routes a query x from any node v to a leaf, returning the path traversed.

Algorithm 2 (QUERY) takes a query x as input and returns at most k memories. The parameter $\epsilon \in [0, 1]$ determines the

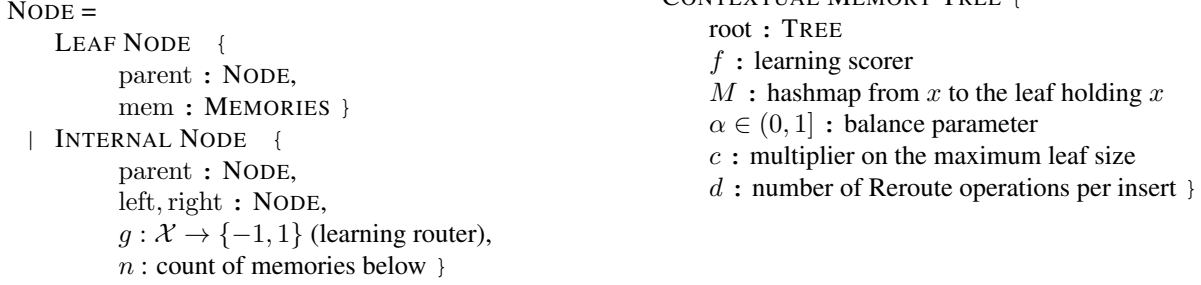


Figure 3: Data structures for internal and leaf nodes (left) and the full contextual memory tree (right).

Algorithm 1 PATH(query x , node v)

```

1: path  $\leftarrow \emptyset$ 
2: while  $v$  is not a leaf do
3:    $a \leftarrow$  if  $v.g(x) > 0$  then right else left
4:   Add  $(v, a, 1)$  to path
5:    $v \leftarrow v.a$ 
6: end while
7: path.leaf  $\leftarrow v$ 
8: return path
    
```

Algorithm 2 QUERY(query x , items to return k , exploration probability ϵ)

```

1: path  $\leftarrow$  PATH( $x$ , root), path =  $\{(v_i, a_i, p_i)\}_{i=1}^N$ 
2:  $q \in_U [0, 1]$ 
3: if  $q \geq \epsilon$  then
4:   return  $(\emptyset, \text{top}_k(\text{path.leaf}, x))$ 
5: else
6:   Pick  $i \in_U \{1, \dots, N + 1\}$ 
7:   if  $i \leq N$  then
8:     Pick  $a' \in_U \{\text{right}, \text{left}\}$ 
9:      $l = \text{PATH}(x, v_i.a')$ .leaf
10:    return  $((v_i, a', 1/2), \text{top}_k(l, x))$ 
11:  else
12:    return  $((\text{path.leaf}, \perp, \perp), \text{rand}_k(\text{path.leaf}, x))$ 
13:  end if
14: end if
    
```

probability of exploration during training. Algorithm 2 first deterministically routes the query x to a leaf and records the path traversed, path. With probability $1 - \epsilon$, we simply return the best memories stored in path.leaf: For a query x and leaf l , we use $\text{top}_k(l, x)$ as a shorthand for the set of $\min\{k, |l.\text{mem}|\}$ memories z in $l.\text{mem}$ with the largest $f(x, z)$, breaking ties randomly. We also use $\text{rand}_k(l, x)$ for a random subset of $\min\{k, |l.\text{mem}|\}$ memories in $l.\text{mem}$.

With the remaining probability ϵ , we uniformly sample a node along path including path.leaf. If we sampled an internal node v , we choose a random action a' and call

Algorithm 3 UPDATE((x, z, r) , (v, a, p))

```

1: if  $v$  is a leaf then
2:    $f.\text{update}(x, z, r)$ 
3: else
4:    $\hat{r} \leftarrow \frac{r}{p}(\mathbf{1}(a = \text{right}) - \mathbf{1}(a = \text{left}))$ 
5:    $y \leftarrow (1 - \alpha)\hat{r} + \alpha(\log v.\text{left}.n - \log v.\text{right}.n)$ 
6:    $v.g.\text{update}(x, \text{sign}(y), |y|)$ 
7: end if
8: Run REROUTE  $d$  times
    
```

path($x, v.a'$) to route x to a leaf. This exploration gives us a chance to discover potentially better memories stored in the other subtrees beneath v , which allows us to improve the quality of the router at node v . We do uniform exploration at a uniformly chosen node but other schemes are possible. If we sampled path.leaf, we return a random set of memories stored in the leaf, in order to update and improve the learning scorer f . The shorter the path, the higher the probability that exploration happens at the leaf.

Algorithm 4 INSERT(node v , memory z , Reroute operations d)

```

1: while  $v$  is not a leaf do
2:    $B = \log v.\text{left}.n - \log v.\text{right}.n$ 
3:    $y \leftarrow \text{sign}((1 - \alpha)v.g(z.x) + \alpha B)$ 
4:    $v.g.\text{update}(z.x, y)$ 
5:    $v.n \leftarrow v.n + 1$ 
6:    $v \leftarrow$  if  $v.g(z.x) > 0$  then  $v.\text{right}$  else  $v.\text{left}$ 
7: end while
8: INSERTLEAF( $v, z$ )
9: Run REROUTE  $d$  times
    
```

After a query for x , we may receive a reward r for a returned memory z . In this case, Algorithm 3 (UPDATE) uses the first triple returned by QUERY to update the router making a randomized decision. More precisely, Algorithm 3 computes an unbiased estimate of the reward difference of the left/right decision which is then mixed with a balance-inducing term on line 5. When randomization occurred at

Algorithm 5 INSERTLEAF(leaf node v , memory z)

```

1:  $v.\text{mem} \leftarrow v.\text{mem} \cup \{z\}$ 
2: if  $|v.\text{mem}| > c \log(\text{root}.n)$  then
3:    $v' \leftarrow$  a new internal node with two new children
4:   for  $z \in v.\text{mem}$  do
5:     INSERT( $v', z, 0$ )
6:   end for
7:    $v \leftarrow v'$ 
8: end if

```

the leaf, the scorer f is updated instead.

The INSERT operation is given in Algorithm 4. It routes the memory z to be inserted according to the query $z.x$ from the root to a leaf using internal learning routers, updating them on descent. Once reaching a leaf node, z is added into that leaf via INSERTLEAF. The label definition on line 3 in INSERT is the same as was used in (Beygelzimer et al., 2009). That use, however, was for a different problem (conditional label estimation) and is applied differently (controlling the routing of examples rather than just advising a learning algorithm). As a consequence, the proofs of correctness given in section 3.1 differ.

When the number of memories stored in any leaf exceeds the log of the total number of memories, a leaf is split according to Algorithm 5 (INSERTLEAF). The leaf node v is promoted to an internal node with two leaf children and a binary classifier g with all memories inserted at v .

Because updates are online, they may result in a lack of self-consistency for previous insertions. This is fixed by REROUTE (Algorithm 7) on an amortized basis. Specifically, after every INSERT operation we call REROUTE, which randomly samples an example from all the examples stored in the tree, extracts the sampled example from the tree, and then re-inserts it. This relies on the REMOVE (Algorithm 6) operation, which finds the location of a memory using the hashmap then ascends to the parent cleaning up accounting. When a leaf node ends up with zero memories, it is removed.

3. Properties

There are five properties that we want CMT to satisfy simultaneously (see Figure 1 (left) for the five properties). Storage (in appendix A.1) and Incrementality (in appendix A.2) are easy observations.

Appendix A.6 shows that in the limit of many REROUTES, self-consistency (defined below) is achieved.

Definition 3.1 A CMT is **self-consistent** if for all z with a unique $z.x$, $z = \text{QUERY}(z.x, 1, 0)$.

Algorithm 6 REMOVE(x)

```

1: Find  $v \leftarrow M(x)$ , leaf containing  $x$ 
2:  $v.\text{mem} \leftarrow v.\text{mem} \setminus \{x\}$ 
3: while  $v$  is not root do
4:   if  $v.n > 0$  then
5:      $v.n \leftarrow v.n - 1$ 
6:      $v \leftarrow v.\text{parent}$ 
7:   else
8:      $v' =$  the other child of  $v.\text{parent}$ .
9:      $v.\text{parent} \leftarrow v'$ 
10:     $v \leftarrow v'$ 
11:  end if
12: end while

```

Algorithm 7 REROUTE()

```

1: Sample  $z \in_U M$ 
2: REMOVE( $z.x$ )
3: INSERT( $\text{root}, z, 0$ )

```

Appendix A.7 shows a learning property: Every internal router asymptotically optimizes to a local maxima of an objective function that mirrors line 5 of UPDATE.

This leaves only logarithmic computational time, which we address next.

3.1. Computational Time

The computational time analysis naturally breaks into two parts, partition quality at the nodes and the time complexity given good partitions. To connect the two, we first define partition quality.

Definition 3.2 A K -balanced partition of any set has each element of the partition containing at least a $1/K$ fraction of the original set.

When partitioning into two sets, $K \geq 2$ is required. Smaller K result in smaller computational complexities at the cost of worse predictive performance in practice.

Define the progressive training error of a learning router g after seeing T examples x_1, \dots, x_T as $p = \frac{1}{T} \sum_{t=1}^T \mathbf{1}[g(x_t) \neq y_t]$, where y_t is the label assigned in line 3 of INSERT, and $g(x_t)$ is evaluated immediately after calling $g.\text{update}(x_t, y_t)$ so a mistake occurs when $g(x_t)$ disagrees with y_t after the update. The next theorem proves a bound on the partition balance dependent on the progressive training error of a node's router and α .

Theorem 3.3 (Partition bound) At any point, a router with a progressive training error of p creates a $\frac{1 + \exp(\frac{1-\alpha}{\alpha})}{(1-p) - (1 + \exp(\frac{1-\alpha}{\alpha}))^{\frac{1}{T}}}$ -balanced partition.

The proof is in appendix A.3, followed by a bound on the depth of K -partition trees in appendix A.4. As long as $(1 - p) > \exp(\frac{1-\alpha}{\alpha}) \frac{1}{T}$ holds, Theorem 3.3 provides a nontrivial bound on partition. Examining limits, when $p = 0$, $\alpha = 1$ and $T = \infty$, we have $K = 2$, which means CMT becomes a perfectly balanced binary tree. If $p = 0.5$ (e.g., g guesses at random), $\alpha = 0.9$ (used in all our experiments) and $T = \infty$, we have $K \leq 4.3$. For any fixed T , a smaller progressive error p and a larger α lead to a smaller K .

Next, we prove that K controls the computational time.

Theorem 3.4 (Computational Time) *If every router g in a CMT with T previous calls to INSERT creates a K -partition, the worst case computation is $O(d(K + c) \log T)$ for INSERT, $O((K + c) \log T)$ for QUERY, and $O(1)$ for UPDATE if all stated operations are atomic.*

The proof is in appendix A.5. This theorem establishes logarithmic time computation given that K -partitions are created. These two theorems imply that the computation is logarithmic time for all learning algorithms achieving a training error significantly better than 1.

4. Experiments

CMT is a subsystem for other learning tasks, so it assists other inference and learning algorithms. We test the application of CMT to three systems, for multiclass classification, multilabel classification, and image retrieval. Many other applications, of course, exist.

Separately, we also ablate various elements of CMT to discover its strengths and weaknesses.

We implemented CMT as a reduction to Vowpal Wabbit’s (Langford et al., 2007) default learning algorithm. Similarly, most baselines are implemented in the same system with a similar or higher level of optimization.

4.1. Application: Online Extreme Multi-Class Classification

Since CMT operates online, we can evaluate its online performance using progressive validation (Blum et al., 1999) (i.e., testing each example ahead of training). Used online, we QUERY for an example, evaluate its loss, then apply UPDATE with the observed loss followed by INSERT of the data point. In a multiclass classification setting, a memory z is a feature vector x and label ω . Given a query x , CMT returns a memory z and receives a reward signal $\mathbf{1}[z.\omega = \omega]$ for update. Finally, CMT inserts (x, ω) .

We test the online learning ability of CMT on two multiclass classification datasets, ALOI (1000 labels with 100 examples per label) and WikiPara 3-shot (10000 labels with 3 examples per label), against two other logarithmic-time on-

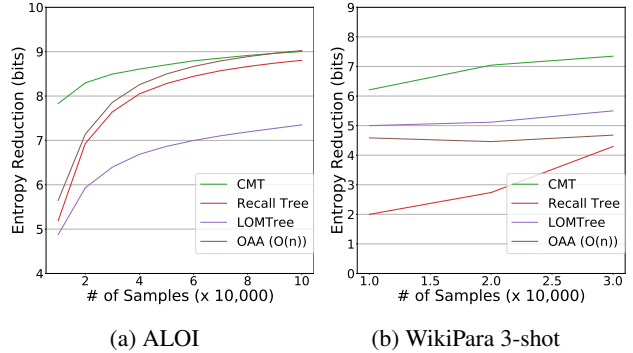


Figure 4: (a) Online progressive performance of CMT with respect to the number of samples on ALOI (a) and WikiPara 3-shot (b). CMT consistently outperforms all baselines.

line multiclass classification algorithms, LOMTree (Choromanska & Langford, 2015) and Recall Tree (Daumé et al., 2017). We also compare against a linear-time online multiclass classification algorithm, One-Against-All (OAA).

Figure 4 summarizes the results in terms of progressive performance. On both datasets, we report entropy reduction from the constant predictor (the higher the better). The entropy reduction of a predictor A from another predictor B is defined as $\log_2(p_A) - \log_2(p_B)$, where p_A and p_B are prediction accuracies of A and B .

Conclusion: CMT greatly outperforms the baselines in the small number of examples per label regime. This appears to be primarily due to the value of explicit memories over learned parameters in this regime.

4.2. Application: Batch Few-shot Multi-Class Classification

We can also use CMT in an offline testing mode as well by using CMT with multiple passes over the the training dataset and testing it on a separate test set. We again use CMT on few-shot multi-class classification, comparing it to LOMTree and Recall Tree.

Starting first with the ALOI dataset, we tested both the unsupervised version (i.e., using only INSERT) and the supervised version (i.e., using INSERT for the first pass, and using UPDATE for subsequent passes). We used three passes for all algorithms. The supervised version of CMT achieved 26.3% test prediction error, outperforming LOMTree (66.7%) and Recall Tree (28.8%). The supervised version of CMT also significantly outperforms the unsupervised one (75.8% error rate), showing the benefit of the UPDATE procedure. Since ALOI has 1000 classes, a constant predictor has prediction error larger than 99%.

We then test CMT on more challenging few-shot multi-class

Approach	RCV1-1K			AmazonCat-13K			Wiki10-31K		
	loss	Test time	Train time	loss	Test time	Train time	loss	Test time	Train time
CMT	2.5	1.4ms	1.9hr	3.2	1.7ms	5.3hr	18.3	25.3ms	1.3hr
OAA	2.6	0.5ms	1.3hr	3.0	8.7ms	15.5hr	20.3	327.1ms	7.2hr

Table 1: Hamming Loss, test time per example (ms), and training time (hr) for multi-label tasks.

classification datasets, WikiPara S -shot ($S = 1, 2, 3$) and ImageNet S -shot ($S = 1, 2, 3, 5$) with only S examples per label. Figure 1 summarizes the statistical performance (entropy reduction compared to a constant predictor) of supervised CMT, unsupervised CMT (denoted as CMT (u)), and the two logarithmic-time baselines. For one-shot experiments (WP 1-s and IN 1-s on Figure 1), CMT outperforms all baselines. The edge of CMT degrades gradually over baselines as S increases (IN S s with $S > 1$ in Figure 1). All details are included in Table 6 in Appendix §B.3.

Conclusion: The high performance of CMT with a small number of examples per label persists in batch training. The remarkable performance of unsupervised CMT over supervised baselines suggests self-consistency can provide nearest-neighbor performance without explicit reward.

4.3. Application: Multi-Label Classification with an External Inference Algorithm

In this set of experiments, instead of using CMT as an inference algorithm, we integrate CMT with an external inference procedure based on One-Against-All. CMT is not aware of the external multi-label classification task, so this is an example of how an external inference algorithm can leverage the returned memories as an extra source of information to improve performance. Here each memory z consists of a feature vector x and label vector $\omega \in \{0, 1\}^M$, where M is the number of unique labels. Given a query x , its ground truth label vector ω , and a memory z , we choose the F1-score between ω and $z.\omega$ as the reward signal. We set k to $c \log(N)$ (i.e., CMT returns all memories in the leaf we reach). Given a query x , with the returned memories $\{z_1, \dots, z_k\}$, the external inference procedure extracts the unique labels from the returned memories and performs a One-Against-Some (OAS) inference (Daumé et al., 2017) using the extracted labels.¹ The external system then calls UPDATE for the returned memories. Since CMT returns logarithmically many memories, we guarantee that the number of unique labels from the returned memories is also logarithmic. Hence augmenting OAS with CMT enables logarithmic inference and training time.

We compare CMT-augmented OAS with a baseline multi-

¹OAS takes x and a small set of candidate labels and returns the labels with a positive score, according to a learned scoring function. After prediction, the OAS predictor receives the true labels y associated with this x and performs an update to its score function based on the true labels and the small candidate label set.

label OAA approach under the Hamming loss. We compare CMT-augmented OAS to OAA on three multi-label datasets, RCV1-1K (Prabhu & Varma, 2014), AmazonCat-13K (McAuley & Leskovec, 2013), and Wiki-31K (Zubiaga, 2012; Bhatia et al., 2015). (The datasets are described in Table 4 in Appendix B.1.) Table 1 summarizes the performance of CMT and OAA. (LOMTree and Recall Tree are excluded because they do not operate in multi-label settings.)

Conclusion: CMT-augmented OAS achieves similar statistical performance to OAA, even mildly outperforming OAA on Wiki10-31K, while gaining significant computational speed up over a vector optimized OAA in training and inference on datasets with a large number of labels (e.g., AmazonCat-13K and Wiki10-31K). This set of experiments shows that CMT-augmented OAS can win over OAA both statistically and computationally for challenging few-shot multi-label datasets with a large number of labels.

4.4. Application: Image Retrieval

Finally, we test CMT on an image retrieval task where the goal is to find an image given a caption. We used three benchmark datasets, (1) UIUC Pascal Sentence Dataset (Rashtchian et al., 2010), (2) Flickr8k dataset (Hodosh et al., 2013), and (3) MS COCO (Lin et al., 2014), with feature representations described in §B.1. Here, a memory z consists of (features of) a caption x and an image ω . Given a query, CMT returns a memory $z = (x, \omega)$. Our reward function is the cosine similarity between the returned memory’s image $z.\omega$, and the ground truth image ω associated with the query x .

To show the benefit of learning in CMT, we compare it to Nearest Neighbor Search (NNS) and a KD-Tree as an Approximate NN data structure on this task, using the Euclidean distance $\|x - z.x\|_2$ in the feature space of captions as the NNS metric.

Both CMT and NNS are tested on a separate test set, with the average reward of the retrieved memory reported.

Table 2 summarizes the speedup over NNS (implemented using a linear scan) and KD-Tree (KD tree implementation from scikit-learn (Pedregosa et al., 2011)). Note that in our datasets, the feature of a query is high dimensional (2^{20}) but extremely sparse. Since KD-Tree cannot take advantage of sparsity, both the construction and inference procedure is extremely slow (even slower than a NNS). We

also emphasize here that a KD-Tree does not operate in an online manner. Hence in our experiments, we have to feed all queries from the entire training dataset to KD-Tree to initialize its construction, which makes it impossible to initialize the run of KD-Tree on MSCOCO.

Conclusion: The difference in reward is negligible (on the order of 10^{-3}) and statistically insignificant. (See Appendix Table 7 for details.) However, CMT is significantly faster.

	CMT	
	unsup	sup
Pascal	5.7 / 9400	1.3 / 2100
Flickr8k	26.0 / 33000	6.0 / 7700
MSCOCO	21.0 / ~	6.5 / ~

Table 2: Speedups over linear NNS (left) and KD-Tree (right), in (unsup)ervised and (sup)ervised mode.

4.5. Ablation Analysis of CMT

We conduct experiments to perform an ablation study of CMT in the context of multi-class classification, where it operates directly as an inference algorithm.

We test the self-consistency property on WikiPara with only one training example per class (see Figure 5a). We ran CMT in an unsupervised fashion, by only calling INSERT and using $-||x - z.x||$ as $f(x, z)$ to select memories at leafs. We report the self-consistency error with respect to the number of REROUTE calls per insertion (parameter d) after four passes over the dataset (tuned using a holdout set). As d increases, the self-consistency error rapidly drops.

To show that UPDATE is beneficial, we use multiple passes to drive the training error down to nearly zero. Figure 5b shows the training error versus the number of passes on the WikiPara one-shot dataset (on the x -axis, we plot the number of additional passes over the dataset, with zero corresponding to a single pass). Note that the training error is essentially equal to the self-consistency error in WikiPara One-shot, hence UPDATE further enhances self-consistency due to the extra REROUTE operations in UPDATE.

To test the effect of the multiplier c (the leaf memories multiplier), we switch to the ALOI dataset (Geusebroek et al., 2005), which has 100 examples per class enabling good generalization. Figure 5c shows that statistical performance improves with inference time and the value of c . In Appendix §B.2, we include plots showing statistical and inference time performance vs c in Figure 6 with inference time scaling linearly in c as expected.

Last, we test CMT on a series of progressively more difficult datasets generated from ALOI via randomly sampling S training examples per label, for S in 1 to 100. ALOI has 1000 unique labels so the number of memories CMT stores

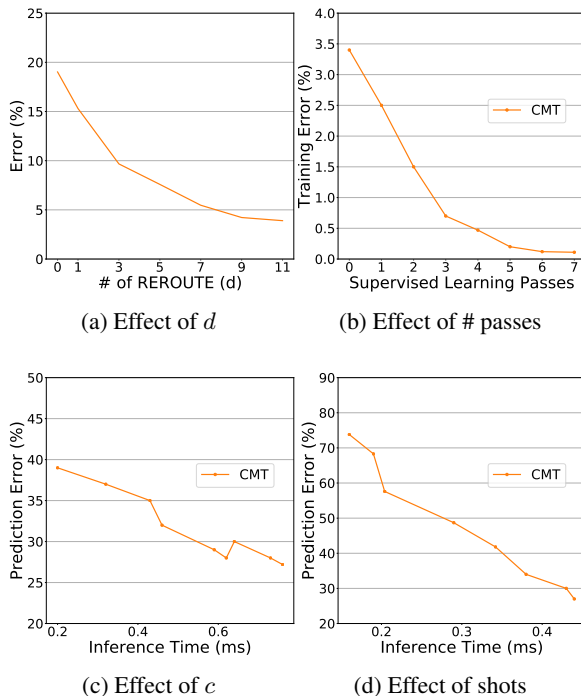


Figure 5: (a) As the number of REROUTE operations increases CMT performs better, asymptoting at 10 on WikiPara one-shot, (b) the effect of the number of UPDATE calls on the training error on WikiPara one-shot, (c) the inference time and prediction error with respect to c on ALOI, and (d) the inference time and prediction error with respect to number of shots on ALOI.

scales as $S \times 1000$, for S -shot ALOI. We fix $c = 4$. Figure 5d shows the statistical performance vs inference time as S varies. The prediction error drops quickly as we increase S . Appendix §B.2 includes detailed plots. Inference time increases logarithmically with S (Figure 7b), matching CMT’s logarithmic time operation theory.

5. Conclusion

CMT provides a new tool for learning algorithm designers by enabling learning algorithms to work with an unsupervised or reinforced logarithmic time memory store. Empirically, we find that CMT provides remarkable unsupervised performance, sometimes beating previous supervised algorithms while reinforcement provides steady improvements.

References

Andrychowicz, M. and Kurach, K. Learning efficient algorithms with hierarchical attentive memory. *CoRR*, abs/1602.03218, 2016. URL <http://arxiv.org/abs/1602.03218>.

Bartl, A. and Spanakis, G. A retrieval-based dialogue system

- utilizing utterance and context embeddings. 2017. URL <http://arxiv.org/abs/1710.05780>.
- Beygelzimer, A., Kakade, S., and Langford, J. Cover trees for nearest neighbor. In *Machine Learning, Proceedings of the Twenty-Third International Conference (ICML 2006), Pittsburgh, Pennsylvania, USA, June 25-29, 2006*, pp. 97–104, 2006. doi: 10.1145/1143844.1143857. URL <http://doi.acm.org/10.1145/1143844.1143857>.
- Beygelzimer, A., Langford, J., Lifshits, Y., Sorkin, G., and Strehl, A. Conditional probability tree estimation analysis and algorithms. In *Proceedings of the Twenty-Fifth Conference on Uncertainty in Artificial Intelligence*, pp. 51–58. AUAI Press, 2009.
- Bhatia, K., Jain, H., Kar, P., Varma, M., and Jain, P. Sparse local embeddings for extreme multi-label classification. In *Advances in Neural Information Processing Systems*, pp. 730–738, 2015.
- Blum, A., Kalai, A., and Langford, J. Beating the hold-out: Bounds for k-fold and progressive cross-validation. In *Proceedings of the twelfth annual conference on Computational learning theory*, pp. 203–208. ACM, 1999.
- Broder, A. Z., Carmel, D., Herscovici, M., Soffer, A., and Zien, J. Y. Efficient query evaluation using a two-level retrieval process. In *Proceedings of the 2003 ACM CIKM International Conference on Information and Knowledge Management, New Orleans, Louisiana, USA, November 2-8, 2003*, pp. 426–434, 2003. doi: 10.1145/956863.956944. URL <http://doi.acm.org/10.1145/956863.956944>.
- Brouwer, L. E. J. ber abbildungen von mannigfaltigkeiten. *Mathematische Annalen*, 71:97–115, 1911.
- Cesa-Bianchi, N. and Lugosi, G. *Prediction, learning, and games*. Cambridge University Press, 2006. ISBN 978-0-521-84108-5.
- Chandar, S., Ahn, S., Larochelle, H., Vincent, P., Tesauro, G., and Bengio, Y. Hierarchical memory networks. *arXiv preprint arXiv:1605.07427*, 2016.
- Choromanska, A. E. and Langford, J. Logarithmic time online multiclass prediction. In *Advances in Neural Information Processing Systems*, pp. 55–63, 2015.
- Dasgupta, S. and Sinha, K. Randomized partition trees for nearest neighbor search. *Algorithmica*, 72(1):237–263, 2015. doi: 10.1007/s00453-014-9885-5. URL <https://doi.org/10.1007/s00453-014-9885-5>.
- Datar, M., Immorlica, N., Indyk, P., and Mirrokni, V. S. Locality-sensitive hashing scheme based on p-stable distributions. In *Proceedings of the 20th ACM Symposium on Computational Geometry, Brooklyn, New York, USA, June 8-11, 2004*, pp. 253–262, 2004. doi: 10.1145/997817.997857. URL <http://doi.acm.org/10.1145/997817.997857>.
- Daumé, III, H., Karampatziakis, N., Langford, J., and Mineiro, P. Logarithmic time one-against-some. *ICML*, 2017.
- Freund, Y. and Schapire, R. E. A decision-theoretic generalization of on-line learning and an application to boosting. *J. Comput. Syst. Sci.*, 55(1):119–139, 1997. doi: 10.1006/jcss.1997.1504. URL <https://doi.org/10.1006/jcss.1997.1504>.
- Geusebroek, J.-M., Burghouts, G. J., and Smeulders, A. W. The amsterdam library of object images. *International Journal of Computer Vision*, 61(1):103–112, 2005.
- Graves, A., Wayne, G., Reynolds, M., Harley, T., Danihelka, I., Grabska-Barwinska, A., Colmenarejo, S. G., Grefenstette, E., Ramalho, T., Agapiou, J., Badia, A. P., Hermann, K. M., Zwols, Y., Ostrovski, G., Cain, A., King, H., Summerfield, C., Blunsom, P., Kavukcuoglu, K., and Hassabis, D. Hybrid computing using a neural network with dynamic external memory. *Nature*, 538(7626):471–476, 2016. doi: 10.1038/nature20101. URL <https://doi.org/10.1038/nature20101>.
- Gu, J., Wang, Y., Cho, K., and Li, V. O. K. Search engine guided non-parametric neural machine translation. In *AAAI*, 2018.
- Hodosh, M., Young, P., and Hockenmaier, J. Framing image description as a ranking task: Data, models and evaluation metrics. *Journal of Artificial Intelligence Research*, 47:853–899, 2013.
- Kaiser, L., Nachum, O., Roy, A., and Bengio, S. Learning to remember rare events. *ICLR*, 2017.
- Karnin, Z. S., Liberty, E., Lovett, S., Schwartz, R., and Weinstein, O. Unsupervised svms: On the complexity of the furthest hyperplane problem. In *COLT 2012 - The 25th Annual Conference on Learning Theory, June 25-27, 2012, Edinburgh, Scotland*, pp. 2.1–2.17, 2012. URL <http://jmlr.org/proceedings/papers/v23/karnin12/karnin12.pdf>.
- Knuth, D. E. *The art of computer programming, Volume I: Fundamental Algorithms, 3rd Edition*. Addison-Wesley, 1997. ISBN 0201896834. URL <http://www.worldcat.org/oclc/312910844>.
- Langford, J., Li, L., and Strehl, A. Vowpal wabbit online learning project, 2007.
- Lin, T.-Y., Maire, M., Belongie, S., Hays, J., Perona, P., Ramanan, D., Dollár, P., and Zitnick, C. L. Microsoft coco: Common objects in context. In *European conference on computer vision*, pp. 740–755. Springer, 2014.
- McAuley, J. and Leskovec, J. Hidden factors and hidden topics: understanding rating dimensions with review text. In *Proceedings of the 7th ACM conference on Recommender systems*, pp. 165–172. ACM, 2013.
- Oquab, M., Bottou, L., Laptev, I., and Sivic, J. Learning and transferring mid-level image representations using convolutional neural networks. In *Computer Vision and Pattern Recognition (CVPR), 2014 IEEE Conference on*, pp. 1717–1724. IEEE, 2014.
- Pedregosa, F., Varoquaux, G., Gramfort, A., Michel, V., Thirion, B., Grisel, O., Blondel, M., Prettenhofer, P., Weiss, R., Dubourg, V., et al. Scikit-learn: Machine learning in python. *Journal of machine learning research*, 12(Oct):2825–2830, 2011.
- Prabhu, Y. and Varma, M. Fastxml: A fast, accurate and stable tree-classifier for extreme multi-label learning. In *Proceedings of the 20th ACM SIGKDD international conference on Knowledge discovery and data mining*, pp. 263–272. ACM, 2014.

- Rae, J., Hunt, J. J., Danihelka, I., Harley, T., Senior, A. W., Wayne, G., Graves, A., and Lillicrap, T. Scaling memory-augmented neural networks with sparse reads and writes. In *NIPS*, 2016.
- Rashtchian, C., Young, P., Hodosh, M., and Hockenmaier, J. Collecting image annotations using amazon’s mechanical turk. In *Proceedings of the NAACL HLT 2010 Workshop on Creating Speech and Language Data with Amazon’s Mechanical Turk*, pp. 139–147. Association for Computational Linguistics, 2010.
- Rastegari, M., Farhadi, A., and Forsyth, D. A. Attribute discovery via predictable discriminative binary codes. In *Computer Vision - ECCV 2012 - 12th European Conference on Computer Vision, Florence, Italy, October 7-13, 2012, Proceedings, Part VI*, pp. 876–889, 2012. doi: 10.1007/978-3-642-33783-3_63. URL https://doi.org/10.1007/978-3-642-33783-3_63.
- Salakhutdinov, R. and Hinton, G. E. Semantic hashing. *Int. J. Approx. Reasoning*, 50(7):969–978, 2009. doi: 10.1016/j.ijar.2008.11.006. URL <https://doi.org/10.1016/j.ijar.2008.11.006>.
- Shrivastava, A. and Li, P. Improved asymmetric locality sensitive hashing (ALSH) for maximum inner product search (MIPS). In *Proceedings of the Thirty-First Conference on Uncertainty in Artificial Intelligence, UAI 2015, July 12-16, 2015, Amsterdam, The Netherlands*, pp. 812–821, 2015.
- Simonyan, K. and Zisserman, A. Very deep convolutional networks for large-scale image recognition. *arXiv preprint arXiv:1409.1556*, 2014.
- Weinberger, K. Q., Blitzer, J., and Saul, L. K. Distance metric learning for large margin nearest neighbor classification. In *Advances in Neural Information Processing Systems 18 [Neural Information Processing Systems, NIPS 2005, December 5-8, 2005, Vancouver, British Columbia, Canada]*, pp. 1473–1480, 2005. URL <http://papers.nips.cc/paper/2795-distance-metric-learning-for-large-margin-nearest-neighbor-classification>.
- Weston, J., Chopra, S., and Bordes, A. Memory networks. *CoRR*, abs/1410.3916, 2014. URL <http://arxiv.org/abs/1410.3916>.
- Xu, L. and Schuurmans, D. Unsupervised and semi-supervised multi-class support vector machines. In *Proceedings, The Twentieth National Conference on Artificial Intelligence and the Seventeenth Innovative Applications of Artificial Intelligence Conference, July 9-13, 2005, Pittsburgh, Pennsylvania, USA*, pp. 904–910, 2005. URL <http://www.aaai.org/Library/AAAI/2005/aaai05-143.php>.
- Zubiaga, A. Enhancing navigation on wikipedia with social tags. *arXiv preprint arXiv:1202.5469*, 2012.

A. Theorems and proofs

A.1. Storage

Bounded storage is an easy desiderata to satisfy.

Claim A.1 For any $T > 0$, a contextual memory tree after T insertions requires only $O(T)$ storage.

Proof: The hashmap is $O(T)$. The number of internal nodes is bounded by the number of leaf nodes. Since every leaf node has at least one unique memory, the storage requirement for internal nodes is $O(T)$, and so is the storage requirement for the leaves. \square

A.2. Incrementality

By observation, all contextual memory tree algorithms are incremental so the overall operation is incremental as long as the underlying learning algorithms for the learning scorer and routers are incremental. In fact, the contextual memory tree is online so long as the underlying learning algorithms are online.

A.3. Partitioning

Here we prove the partition bound (Theorem 3.3).

Proof: Let R_t and L_t be the number of memories in the right and left subtree respectively, at the start of round t for which we are proving the theorem.

Observe that if

$$\alpha \log \frac{L_t}{R_t} > 1 - \alpha,$$

or, equivalently, if

$$\frac{L_t}{R_t} > e^{\frac{1-\alpha}{\alpha}},$$

or equivalently, if

$$\frac{L_t}{N_t} > \frac{1}{1 + \exp(1 - \frac{1}{\alpha})}, \quad (1)$$

where $N_t = R_t + L_t$ we always have $y = 1$.

A symmetric argument shows that if

$$\frac{R_t}{N_t} > \frac{1}{1 + \exp(1 - \frac{1}{\alpha})}, \quad (2)$$

we always have $y = -1$.

Denote $\kappa = \frac{1}{1 + \exp(1 - \frac{1}{\alpha})}$. Note that $\kappa < 1$. We claim that for any t , we have

$$R_t \leq (1 - p_t)\kappa N_t + (1 - \kappa) + p_t N_t, \text{ and } L_t \leq (1 - p_t)\kappa N_t + (1 - \kappa) + p_t N_t, \quad (3)$$

where p_t is the progressive training error at the beginning of round t . We prove the claim by induction on t . The base case holds by inspection, assuming $L_2 = R_2 = 1$ and $p_2 = 0$ (i.e., by simply initializing all leaf with a default example).

Assume that the claim holds for step t , and consider step $t + 1$.

Below we first consider the first case: (1) $R_t > \kappa N_t$.

Note that in this case, we always have $y = -1$. Whether or not we route the example to the left depends on whether or not the router makes a post-update mistake. Hence, we discuss two sub-cases below.

(a) The router does not make a mistake here. In this case, the router routes the example to the left. Since no mistake happens in this round, we have $p_{t+1}N_{t+1} = p_t N_t$, i.e., the total number of mistakes remain the same. Then, we have:

$$R_{t+1} = R_t \leq (1 - p_t)\kappa N_t + (1 - \kappa) + p_t N_t \leq (1 - p_{t+1})\kappa N_{t+1} + (1 - \kappa) + p_{t+1} N_{t+1}, \quad (4)$$

where the inequality comes from the fact that $N_{t+1} = N_t + 1 > N_t$.

Now we consider the second sub-case here.

(b) The router does make a mistake. In this case, the router routes the example to the right. Note that in this case, we have $p_{t+1}N_{t+1} = p_tN_t + 1$, i.e., the total number of mistakes increases by one. Hence, we have for R_{t+1} :

$$\begin{aligned}
 R_{t+1} &= R_t + 1 \leq (1 - p_t)\kappa N_t + (1 - \kappa) + p_tN_t + 1 \\
 &= \kappa N_t - \kappa p_t N_t + (1 - \kappa) + p_tN_t + 1 \\
 &= \kappa N_t - \kappa p_{t+1}N_{t+1} + \kappa + (1 - \kappa) + p_tN_t + 1 \\
 &= \kappa N_{t+1} - \kappa p_{t+1}N_{t+1} + (1 - \kappa) + p_{t+1}N_{t+1},
 \end{aligned} \tag{5}$$

where the second equality uses the fact that $\kappa p_{t+1}N_{t+1} = \kappa p_tN_t + \kappa$.

With case (a) and case (b), we can conclude that for case (1) where $R_t > \kappa N_t$, we have:

$$R_{t+1} \leq (1 - p_{t+1})\kappa N_{t+1} + (1 - \kappa) + p_{t+1}N_{t+1}. \tag{6}$$

Now we consider the second case (b): $R_t \leq \kappa N_t$. In this case, regardless of where the example routes, we always have:

$$R_{t+1} \leq R_t + 1 \leq \kappa N_t + 1 = \kappa(N_{t+1} - 1) + 1 = \kappa N_{t+1} + 1 - \kappa. \tag{7}$$

Note that since $\kappa < 1$, we must have $p_{t+1}N_{t+1} \geq p_{t+1}\kappa N_{t+1}$. Hence we have

$$\begin{aligned}
 R_{t+1} &\leq \kappa N_{t+1} + 1 - \kappa \\
 &\leq \kappa N_{t+1} + 1 - \kappa + p_{t+1}N_{t+1} - \kappa p_{t+1}N_{t+1} = (1 - p_{t+1})\kappa N_{t+1} + (1 - \kappa) + p_{t+1}N_{t+1}.
 \end{aligned} \tag{8}$$

With case (1) and case (2), we can conclude that for R_{t+1} , we always have:

$$R_{t+1} \leq (1 - p_{t+1})\kappa N_{t+1} + (1 - \kappa) + p_{t+1}N_{t+1}. \tag{9}$$

A symmetric argument implies

$$L_{t+1} \leq (1 - p_{t+1})\kappa N_{t+1} + (1 - \kappa) + p_{t+1}N_{t+1}. \tag{10}$$

By induction, we prove our claim.

Now given $L_t \leq (1 - p_t)\kappa N_t + (1 - \kappa) + p_tN_t$, we divide N_t on both sides to get:

$$L_t/N_t \leq (1 - p_t)\kappa + \frac{1 - \kappa}{N_t} + p_t. \tag{11}$$

Multiplying both sides by -1 and adding 1, we get:

$$\begin{aligned}
 1 - L_t/N_t &= \frac{R_t}{N_t} \geq 1 - (1 - p_t)\kappa + \frac{\kappa - 1}{N_t} - p_t \\
 &= (1 - p_t) - (1 - p_t)\kappa + \frac{\kappa - 1}{N_t} \\
 &= (1 - p_t)(1 - \kappa) + \frac{\kappa - 1}{N_t}.
 \end{aligned} \tag{12}$$

As $\kappa > 0$, we get:

$$R_t/N_t \geq (1 - p_t)(1 - \kappa) - \frac{1}{N_t}. \tag{13}$$

By symmetry, we have:

$$L_t/N_t \geq (1 - p_t)(1 - \kappa) - \frac{1}{N_t}. \tag{14}$$

Substituting κ in, we get:

$$\min\{L_t/N_t, R_t/N_t\} \geq (1 - p_t) \frac{1}{\exp(\frac{1-\alpha}{\alpha}) + 1} - \frac{1}{N_t}. \tag{15}$$

□

A.4. Depth of K -partitions

Next we prove a depth bound given K -partitions.

Lemma A.2 *A tree on T points with a K -partition at every internal node has depth at most $K \log T$.*

Proof: By assumption, each internal node routes at least a $1/K$ fraction of incident points in either direction, hence at most a $1 - 1/K$ fraction of points are routed the other direction. As a consequence, at a depth d a node has at most $t(1 - 1/K)^d$ memories beneath it. The deepest internal node in the tree satisfies:

$$T(1 - 1/K)^d \geq 1$$

rearranging, we get:

$$T \geq \left(\frac{1}{1 - 1/K} \right)^d$$

Taking the log of both sides, we get:

$$\log T \geq d \log \left(\frac{1}{1 - 1/K} \right)$$

which implies

$$d \leq \frac{\log T}{\log \left(\frac{1}{1 - 1/K} \right)}.$$

Using $-\log(1 - x) \geq x$ for $0 \leq x < 1$, we get

$$d \leq K \log T.$$

□

A.5. Computational bound proof

Now we prove Theorem 3.4.

Proof: We assume that d is constant. From the depth bound, REMOVE is $O(K \log T)$. INSERTLEAF is $O(1)$ if the guard on line 2 is false. If the guard is true, then we know that $|v.m| > c \log T$ and $|v.m| - 1 \leq c \log T$ since otherwise it would have been triggered on a previous insertion. Hence, line 5 executes $O(c \log T)$ times, with each invocation of INSERT taking $O(1)$ time in this case as the while loop in line 1 is executed only once.

INSERT($\cdot, \cdot, 0$) takes $O((K + c) \log T)$ from the depth bound and the complexity of INSERTLEAF. Thus the computational complexity of REROUTE is $O((K + c) \log T)$. UPDATE takes $O(1)$ time, followed by d invocations of REROUTE, making it $O((K + c) \log T)$ time as well. INSERT(\cdot, \cdot, d) takes $O((K + c) \log T)$, followed by d invocations of REROUTE, making its total complexity $O((K + c) \log T)$.

QUERY calls PATH at most twice and then pays $O(c \log T)$ computation to find the top k memories for the query. The complexity of PATH is $O(K \log T)$, making the overall complexity of QUERY $O((K + c) \log T)$. □

A.6. Self-Consistency

Let us recall the definition of self-consistency.

Definition A.3 *A CMT is self-consistent if for all z with a unique $z.x$, $z = \text{QUERY}(z.x, 1, 0)$.*

It is easy to see that self-consistency holds for any z immediately after insertion.

Lemma A.4 *If $z = \arg \max_{z'} f(z.x, z')$, then $z = \text{QUERY}(z.x, 1, 0)$ immediately after INSERT(root, $z, 0$).*

Proof: By construction, the updates in line 4 of INSERT do not affect the routers at nodes closer to the root. Therefore, since INSERT line 6 and PATH line 3 are identical, both INSERT and QUERY walk through the same internal nodes. At INSERTLEAF, the last execution of line 5 is for z and hence any newly created internal node also routes in the same direction. Once a leaf is reached, $z = \arg \max_{z'} f(z.x, z')$ implies the claim follows. □

Achieving self-consistency for all z simultaneously is more difficult since online updates to routers can invalidate pre-existing self-consistency. Nevertheless, the combination of the REROUTE operation and the convergence of learning algorithms at internal nodes leads to asymptotic self-consistency.

Definition A.5 *A convergent learning algorithm satisfies, for all input distributions D and all update sequences,*

$$\mathbf{P}_{x \sim D}[g_t(x) \neq g_{t-1}(x)] = 0,$$

in the limit as $t \rightarrow \infty$.

Restated, a convergent learning algorithm is one that disturbs fewer predictions the more updates that it gets. This property is an abstraction of many existing update rules with decaying learning rates.

Theorem A.6 *For all contextual memory trees T , if $z = \arg \max_{z'} T.f(z.x, z')$ for all z , and all routers g are convergent under the induced sequence of updates, then in the limit as $T.d \rightarrow \infty$, T is self-consistent almost surely.*

Proof: The proof operates level-wise. The uniform REROUTE operation and the fact that the learning algorithm at the root is convergent by assumption guarantees that the root eventually routes in a self-consistent fashion almost surely. Once the root converges, the same logic applies recursively to every internal node, for the distribution of memories induced at the node. To finish the proof, we just use the assumption that $z = \arg \max_{z'} f(z.x, z')$. \square

Asymptotic self-consistency is a relatively weak property so we also study self-consistency empirically in section 4.5.

A.7. Learning

Finding a good partition from a learning perspective is plausibly more difficult than finding a good classifier. For example, in a vector space finding a partition with a large margin which separates input points into two sets each within a constant factor of the original in size is an obvious proxy. The best results for this problem (Xu & Schuurmans, 2005; Karnin et al., 2012) do not scale to large datasets or function in an online fashion.

For any given node we have a set of incident samples which cause updates on INSERT or UPDATE. Focusing on UPDATE at a single node, the natural function to optimize is a form of balanced expected reward. If r_a and p_a are the rewards and probabilities of taking action a , then a natural objective is:

$$\arg \max_g E_{x \sim D} (1 - \alpha) r_{g(x)} - \alpha \log p_{g(x)}^g \quad (16)$$

where $p_a^g = \Pr_{x \sim D}(g(x) = a)$ is the probability that g chooses direction a as induced by samples over x . This objective both maximizes reward and minimizes the frequency of the chosen action, implying a good solution sends samples in both directions.

The performance of the partitioner is dependent on the classifier g which optimizes importance weighted binary classification. In particular, we evaluate the performance of g according to:

$$\hat{E}_{x,y,i} I(g(x) \neq y)$$

with the goal of g minimizing the empirical importance weighted loss over observed samples.

Next we prove a basic sanity check theorem about the asymptotics of learning a single node. For this theorem, we rely upon the notion of a no-regret (Cesa-Bianchi & Lugosi, 2006) g which is also convergent. Common no-regret algorithms like Hedge (Freund & Schapire, 1997) are also convergent for absolutely continuous D generating events. The following theorem relies on the

Theorem A.7 *For all absolutely continuous distributions D over updates with $d = 0$ reroutes and for all compact convergent no-regret g :*

$$\lim_{t \rightarrow \infty} g_t$$

exists and is a local maxima of (16).

The proof is in Appendix A.8. Here, convergent g is as defined in section A.6 and compact g refers to the standard definition of a compact space for the parameterization of g .

It's important to note that the $d = 0$ requirement is inconsistent with the $d \rightarrow \infty$ requirement for self-consistency. This tradeoff is fundamental: a learning process that is grounded in unsupervised updates (as for self-consistency) is fundamentally different from a learning process grounded in rewards (as for the learning update). If these two groundings happen to agree then compatibility exists as every unsupervised update is consistent with a reward update.

This theorem shows that the optimization process eventually drives to a local maxima of (16) providing a single node semantics. Since every node optimizes independently, the joint system therefore eventually achieves convergence over 1-step routing deviations.

A.8. Learning proof

Proof: Consider without loss of generality the root node of the tree, and then apply this argument recursively.

Since g is no-regret the g minimizing (16) for any observed p eventually wins. Since the D producing updates is absolutely continuous, convergence of g implies convergence of p and the g, p system is compact since g is compact and p is compact. Given this, a g, p pair maps to a new g, p pair according to the dynamics of the learning algorithm.

Brouwer's fixed point theorem (Brouwer, 1911) hence implies that there exists a g, p pair which is a fixed point of this process. Since g is no-regret, the system must eventually reach such a fixed point (there may be many such fixed points in general).

Contextual Memory Tree

For a given g , let $\Phi^{(g)} = E_{x \sim D} \left[(1 - \alpha)r_{g(x)} - \alpha \log p_{g(x)}^g \right]$ be the objective in equation (16) and define

$$\begin{aligned} r_{\text{Left}}^{(g)} &= (1 - \alpha)r_{\text{Left}} - \alpha \log p_{\text{Left}}^g \\ r_{\text{Right}}^{(g)} &= (1 - \alpha)r_{\text{Right}} - \alpha \log p_{\text{Right}}^g. \end{aligned}$$

Using this definition, we can define:

$$\begin{aligned} y^{(g)} &= r_{\text{Right}}^{(g)} - r_{\text{Left}}^{(g)} \\ &= (1 - \alpha)(r_{\text{Right}} - r_{\text{Left}}) - \alpha(\log p_{\text{Right}}^g + \log p_{\text{Left}}^g) \\ &= (1 - \alpha)(r_{\text{Right}} - r_{\text{Left}}) + \alpha \log \frac{p_{\text{Left}}^g}{p_{\text{Right}}^g} \\ &\stackrel{\text{a.s.}}{=} (1 - \alpha)(r_{\text{Right}} - r_{\text{Left}}) + \alpha \lim_{\substack{t \rightarrow \infty \\ S \sim D^t}} \log \frac{\sum_{x \in S} I(g(x) = \text{Left})}{\sum_{x \in S} I(g(x) = \text{Right})}. \end{aligned}$$

Assume wlog that $r_{\text{Right}}^{(g)} > r_{\text{Left}}^{(g)}$ such that $|y^{(g)}| = y^{(g)}$. Examining Line 5 of UPDATE, for a fixed g (i.e. $g.\text{update}()$ has converged), taking expectations wrt p over a , and denoting H as the complete empirical history of the node,

$$\begin{aligned} E_p y &= (1 - \alpha) E_{a \sim \bar{p}} \left(\frac{r_{\text{Right}} I(a = \text{Right})}{p(\text{Right})} - \frac{r_{\text{Left}} I(a = \text{Left})}{p(\text{Left})} \right) + E_{x \sim D} \log \frac{\sum_{x \in H} I(g(x) = \text{Left})}{\sum_{x \in H} I(g(x) = \text{Right})} \\ &\stackrel{t \rightarrow \infty}{=} (1 - \alpha)(r_{\text{Right}} - r_{\text{Left}}) + E_{\substack{x \sim D \\ S \sim D^t}} \log \frac{\sum_{x \in S} I(g(x) = \text{Left})}{\sum_{x \in S} I(g(x) = \text{Right})}. \end{aligned}$$

In other words, $\lim_{t \rightarrow \infty} E_p y \stackrel{\text{a.s.}}{=} y^{(g)}$. The expected loss of g then converges to:

$$E \left[|y^{(g)}| I(g(x) \neq \text{sign}(y^{(g)})) \right] \stackrel{\text{a.s.}}{=} \Phi^{(g)}$$

proving the theorem. □

B. Experimental Details

B.1. Datasets

dataset	task	classes	examples
ALOI	Visual Object Recognition	10^3	10^5
WikiPara (S -shot)	Language Modeling	10^4	$S \times 10^4$
ImageNet (S -shot)	Visual Object Recognition	2×10^4	$2S \times 10^4$
Pascal	Image-Caption Q&A	/	10^3
Flickr-8k	Image-Caption Q&A	/	8×10^3
MS COCO	Image-Caption Q&A	/	8×10^4

Table 3: Datasets used for experimentation on multi-class and Image Retrieval

dataset	# Training	# test	# Categories	# Features	Avg # Points/Label	Avg # Labels/Point
RCV1-2K	623847	155962	2456	47236	1218.56	4.79
AmazonCat-13K	1186239	306782	13330	203882	448.57	5.04
Wiki10-31K	14146	6616	30938	101938	8.52	18.64

Table 4: Extreme Multi-Label Classification datasets used for experimentation

Table 3 summarizes the datasets used in Multi-class classification and image retrieval experimentations. ALOI (Geusebroek et al., 2005) is a color image collection of one-thousand small objects. We use the same train and test split and feature representation as Recall Tree

Contextual Memory Tree

	# unsupervised passes	# supervised passes	c	d	α
ALOI	1	2	4	5	0.1
Few-shot WikiPara	1	1	4	5	0.9
Few-shot ImageNet	1	1	4	3	0.9
RCV1-1K	1	3	2	3	0.9
AmazonCat-13K	1	3	2	3	0.9
Wiki10-31K	1	3	2	3	0.9
Pascal	1	1	10	1	0.9
Flickr	1	1	10	1	0.9
MS COCO	1	1	10	1	0.9

Table 5: Key parameters used for CMT for our experiments

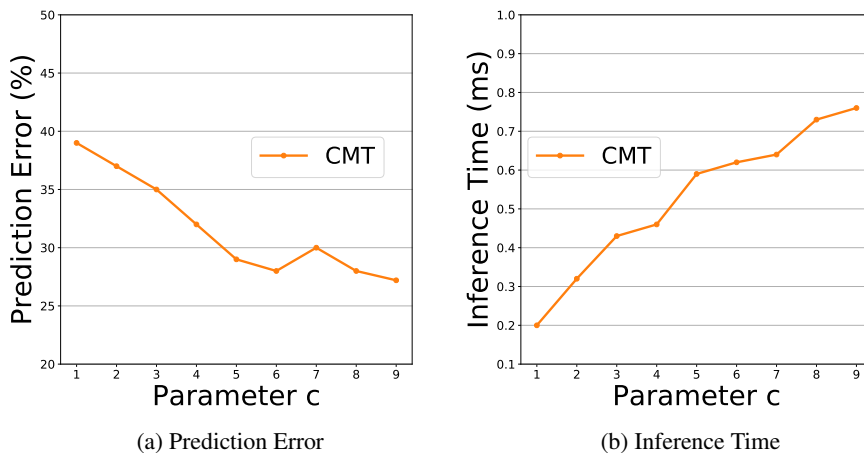


Figure 6: Performance and inference time of CMT versus the number of examples per leaf

(Daumé et al., 2017). The few-shot ImageNet datasets are constructed from the whole ImageNet that has 20,000 classes and 10^7 training examples. We use the same train and test split as Recall Tree (Daumé et al., 2017). The features of images are extracted from intermediate layers of a convolutional neural network trained on the ILSVRC2012 (Oquab et al., 2014). To construct a S -shot ImageNet dataset, we randomly sample S training examples for each class. A S -shot ImageNet dataset hence has a $20000 \times S$ many training examples.

Pascal sentence dataset consists of 1000 pairs of image $I \in \mathbb{R}^{300 \times 180}$ and the corresponding description of the image. We compute HoG feature y for each image I and token occurrences $y \in \mathbb{R}^{20}$ for each description using Scikit-learn’s Hashing functionality. The resulting feature x is high dimensional but extremely sparse. We randomly split the dataset into a training set consisting of 900 pairs of images and their descriptions and a test set with the remaining data. A memory $z = (x, y)$ here consists of the image feature y and the descriptions’ feature x . During inference time, given a query x (i.e., a description of an unknown image), CMT retrieves a memory $z' = (x', y')$, such that the image y' associated with the memory z' is as similar to the unknown image associated with the test query x . Given two memories z and z' , the reward signal is defined as $r(z_y, z'_y) = \langle z_y, z'_y \rangle$. The Flickr8k dataset consists of 8k images and 5 sentences descriptions for each image. Similar to Pascal, we compute HoG feature y for each image and hashing feature x for its 5-sentence description. The MS COCO image caption dataset consists of 80K images in training set, 4000 images in validation set and testing set. We extract image feature y from a fully connected layer in a VGG-19 (Simonyan & Zisserman, 2014) pre-trained on ILSVRC2012 dataset. We use hashing feature x for image captions.

Table 4 summarizes the datasets used for multi-label classification task. All three datasets are obtained from the Extreme Classification Repository (<http://manikvarma.org/downloads/XC/XMLRepository.html>).

All datasets that we used throughout this work are available at (url will be provided here).

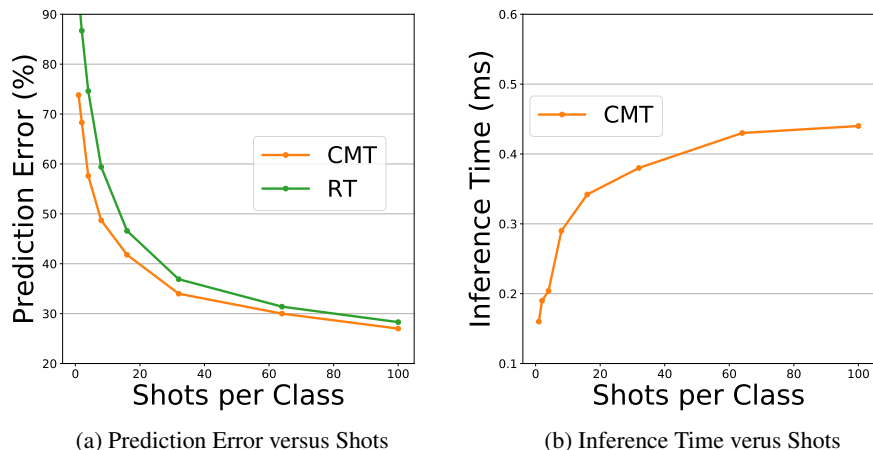


Figure 7: Performance (a) and inference time (b) of CMT versus the number of training examples per label in ALOI (i.e., shots S).

B.2. Extra Plots in Sec. 4.5

Figure 6 shows the detailed plots of CMT’s statistical performance (a) and inference performance (b) with respect to parameter c (i.e., the maximum number of memories per leaf: $c \log(N)$). As shown in Figure 6 (b), the inference time increases almost linear with respect to c , which is expected as once we reach a leaf, we need to scan all memories stored in that leaf.

Figure 7 shows the detailed plots of CMT’s statistical performance (a) and inference time (b) with respect to the number of shots (i.e., number of training examples for each class) in ALOI. Note that ALOI has in total 1000 classes and hence for ALOI S -shot, we will have in total $S \times 1000$ examples. Namely as S increases, CMT has more memories to store. We vary S from 1 to 100. Figure 7a shows the performance of CMT improves quickly as S increases (e.g., dataset becomes easier to learn). Also CMT consistently outperform Recall Tree, with larger margin at fewer shots. From Figure 7 (b), we see that the inference time increases sublinearly with respect to the number of shots (i.e., the number of total memories stored in CMT), which is also expected, as we show that the depth of CMT and the number of memories per leaf are logarithmic with respect to the size of CMT.

B.3. Few-shot Extreme Multi-class Classification Details

Table 6 shows the detailed prediction error and inference time of CMT and other baselines. For ALOI, we briefly tuned the parameters of CMT based on a set of holdout training data, and for few-shot WikiPara (and few-shot ImageNet), we briefly tuned the parameters of CMT using the one-shot dataset on hold-out dataset and then simply just use the same set of parameters across all other few-shot datasets. The detailed key parameters can be found in Table 5.

One interesting observation from Table 6 is that CMT can outperform even OAA at the one-shot WikiPara experiment. All the datasets have same number of examples per class and hence a constant predictor (i.e., prediction by majority) would have prediction accuracy at $1/(\# \text{ of classes})$.

B.4. Multi-Label Classification

The key parameters we used to conduct our multi-label experiments are summarized in Table 5. We briefly tuned the number of supervised passes and α on holdout training datasets and picked a set of parameters that worked well for all datasets in general. We did not tune parameters c and d . The results are summarized in table 1.

B.5. Image Retrieval

For Pascal and Flickr8k, we randomly split the dataset into a pair of training set and test set. We create 5 random splits, and use one split for tuning parameters for CMT. For MS COCO, we use the default training, validation, and test split, and tune parameters on validation set.

For image retrieval applications, the key parameters used by CMT are summarized in Table 5, and the detailed performances of CMT and NN are summarized in Table 7. For Pascal and Flickr8k, since we have 5 training/test split, we report mean and standard deviation.

In this set of experiments, for CMT, during training we set k to be $c \log(N)$, i.e., we returned all memories stored in a single leaf to get reward signals to update f . During testing, for both CMT and NN, we report the average reward of the top returned memory on given test

Contextual Memory Tree

		CMT (u)	CMT	LOMTree	Recall Tree	OAA
ALOI	Test Error	75.8	26.3	66.7	28.8	21.7
	Test Time	0.27	0.15	0.01	0.02	0.05
WikiPara (1-shot)	Test Error	97.3	96.7	98.2	97.1	98.2
	Test Time	0.3	0.3	0.1	0.1	0.9
WikiPara (2-shot)	Test Error	96.3	96.0	96.7	94.0	95.6
	Test Time	0.4	0.4	0.1	0.1	1.1
WikiPara (3-shot)	Test Error	96.1	95.7	96.1	92.0	92.8
	Test Time	0.5	0.3	0.1	0.1	1.1
ImageNet (1-shot)	Test Error	98.8	98.7	99.8	99.7	98.0
	Test Time	9.6	8.2	1.0	3.3	112.4
ImageNet (2-shot)	Test Error	98.7	98.3	99.6	99.3	97.0
	Test Time	11.7	8.6	1.2	3.3	112.0
ImageNet (3-shot)	Test Error	98.6	98.1	99.4	98.9	96.2
	Test Time	9.8	8.5	4.6	3.3	109.0
ImageNet (5-shot)	Test Error	98.4	97.9	99.2	98.6	95.3
	Test Time	12.5	11.6	1.3	4.0	110.4

Table 6: Prediction error (%) and inference time (ms) of different multi-class classification algorithms on few-shot extreme multi-class classification datasets.

		CMT (u)	CMT	NN	KD-Tree w/ PCA
Pascal	Test Reward	0.680±0.008	0.694±0.010	0.683 ±0.013	0.675 ±0.013
	Test Time (ms)	0.13	0.58	0.74	0.002
Flickr8k	Test Reward	0.733±0.004	0.740±0.002	0.736 ±0.003	0.733 ± 0.002
	Test Time (ms)	0.23	1.0	6.0	0.002
MS COCO	Test Reward	0.581	0.584	0.585	0.574
	Test Time (ms)	0.590	1.90	12.4	35.4

Table 7: Performance (average reward % and time *ms*) of different approaches on image retrieval tasks.

sets.

Table 7 summarizes the performance of CMT, NN and KD-Tree operating on a low dimension feature of the query computed from the randomized PCA algorithm from sklearn. We choose the reduced dimension of the feature such that the total PCA time plus the KD-Tree construction time is similar to the time of unsupervised CMT construction time (in Pascal, the reduced dimension is 20; in Flickr8k, the reduced dimension is 200; in MSCOCO, the reduced dimension is 200). Note that on Pascal and Flickr8k, CMT slightly outperforms NN in terms of average reward on test sets, indicating the potential benefit of learned memories. CMT statistically outperforms KD-tree operated on the low dimensional feature computed from PCA.